Available online at www.sciencedirect.com
ScienceDirect
Fuel 86 (2007) 410–417
FUEL
www.fuelfirst.com

Prediction of gaseous products from biomass pyrolysis through combined kinetic and thermodynamic simulations

Dong Ho Lee [a], Haiping Yang [a,b], Rong Yan [a,*], David Tee Liang [a]

[a] *Institute of Environmental Science and Engineering, Nanyang Technological University, Innovation Center, Block 2 Unit 237, 18 Nanyang Drive, Singapore 637723, Singapore*
[b] *National Laboratory of Coal Combustion, Huazhong University of Science and Technology, Wuhan 430074, PR China*

Received 13 December 2005; received in revised form 5 June 2006; accepted 18 July 2006
Available online 5 September 2006

Abstract

Due to the nonhomogeneous characteristics of biomass constituent, it has been known to be difficult to apply directly any simulation work to the pyrolysis of biomass for a precise prediction of gaseous products. In this study, two computation codes (HSC Chemistry for thermodynamic and Sandia PSR for kinetic simulations) were employed, to consider the integrated effects of thermodynamic and kinetic phenomena occurring in biomass pyrolysis on the distribution of gaseous products. The principle of simulation applied in this study was to extract substitutable gas phase compositions from HSC calculations, which were predicted thermodynamically. Then, the gas phase compositions were inputted into the Sandia PSR code to consider the potential constrains of kinetics involving in the pyrolysis and finally to get the distributions of gas products which should be closer to the realistic situation. Palm oil wastes, a local representative biomass, were studied as sample biomass. The gaseous products obtained from HSC calculations were mainly H_2, CO_2, CO, CH_4 and negligible C_{2+} hydrocarbons. After applying these products into PSR program, the final products developed into H_2, CO_2, CO, CH_4, C_2H_2, C_2H_4, C_2H_6 and C_3H_8 which are more realistic products in the modern fast pyrolysis.

Keywords: Palm oil wastes; Simulation; Gas products

1. Introduction

Pyrolysis is currently one of the most promising thermochemical conversion techniques for recovering energy from biomass. Palm oil wastes are local representative biomass and our previous studies reveal that they are ideal sources of renewable energy [1]. The main products from biomass pyrolysis could be liquid oil, solid charcoal and gases in different proportions, depending on the operation conditions. Recently, research interest focuses on the distribution of various gas products from pyrolysis of biomass, aiming to improve the yield of clean energy such as hydrogen [1–3].

Numerous models [4–7] have so far been developed to describe the pyrolysis of biomass; they are mainly based on considerations of kinetics, heat and/or mass transport. However, these models contain parameters, which make them difficult to apply to different reactors to predict the gas product distribution. Models based on thermodynamic equilibrium calculations [7–12] are independent of the reactor. Nevertheless, thermodynamic equilibrium may not be achieved particularly at low temperatures and as such the calculations may not represent the real situation when kinetic constraints become the major factor. Thermodynamic calculations have widely been used in predicting thermal conversions of methane, plastics and coal. As for biomass, it has mostly been used in combustion or gasification processes and only recently it has been used in biomass pyrolysis [4] with focus on the release of the elements K and Cl, rather than the main gaseous products.

More details of predicting biomass pyrolysis using commercial computation approaches are iterated here.

---

[*] Corresponding author. Tel.: +65 67943244; fax: +65 67921291.
E-mail address: ryan@ntu.edu.sg (R. Yan).

0016-2361/$ - see front matter © 2006 Elsevier Ltd. All rights reserved.
doi:10.1016/j.fuel.2006.07.020

de Bruyn Kops and Malte [13] used a commercial combustion software FLUENT to search for the best way to reduce emission from wood dust combustion. In their study the wood particles were considered to break down during the devolatilization process into char and wood volatiles, and the simulation work only utilized the volatile part of wood. Philippe and Raphael carried analysis of a biomass gasifier using ASPEN PLUS software which is based on a minimization of Gibbs free energy at equilibrium [14]. This implies that the residence time is long enough to allow the chemical reactions to reach an equilibrium state. However this assumption of equilibrium is rarely reached in real gasifiers. Baumlin et al. used a continuous self-stirred tank reactor (CSSTR), which is alternatively referred to perfectly stirred reactor, for biomass gas pyrolysis [15]. The aim of their study was to report the experimental results obtained on the thermal cracking of vapors produced by biomass pyrolysis. There are other reports concerning about hydrocarbon pyrolysis, in terms of biomass pyrolysis modeling by TGA [2,16], developing reduced kinetic mechanism [17], general biomass mechanism overview [18], and gaseous fuel pyrolysis modeling [19–21].

Sandia perfectly stirred reactor (PSR) code [22] is a computer program that predicts the steady-state temperature and species composition of gaseous mixture in a perfectly stirred reactor. The reactor is characterized by a reactor volume, residence time or mass flow rate, heat loss or temperature, and incoming temperature and mixture composition. The PSR code is originally developed for combustion of gases, but applying this code together with HSC thermodynamic software and without oxygen it becomes suitable for pyrolysis of biomass, which is assumed to instantly vaporize into a gas mixture. So far, there has been no direct application of Sandia National Laboratories PSR code to biomass pyrolysis appeared in the literatures. One PSR application to pyrolysis developed by Zhou and Mahalingam was in the examination that fuel supply to the largely gases flames in an intense wildland fire is primarily a result of pyrolysis of cellulose in a live wood [23].

In our previous study [2], biomass pyrolysis was conducted in a thermogravimetric analyser coupled with Fourier transform infrared analysis (TGA–FTIR) and a thermodynamic calculation (HSC) [24] was used to predict the distribution of gases products at different temperature. The major finding was significance of temperature influence on pyrolysis of palm oil wastes, particularly on gas product distribution. The difference patterns related to pyrolysis rate and gas evolving profile at low (<355 °C) and high temperatures (>355 °C) are observed and it indicates the different reaction pathway involved. However, thermodynamic calculation does not consider any kinetic constrains. Due to the deficiency of kinetic characteristics of HSC calculations, the yielded products overlooked gases like C_2H_2, C_2H_4, C_2H_6, and C_3H_8, which appear in modern fast biomass pyrolysis process [25]. Moreover, the composition of gaseous products predicted by HSC thermodynamics might not be true in the cases where kinetic phenomena play a role.

The present study implements a Sandia combustion code perfectly stirred reactor (PSR) [22] to simulate more realistic final gas yields using the results obtained from HSC of the previous study from which only the predicted predominant species were used, based on a series of proposed reactions. By combining HSC and PSR calculations, the predictions of HSC now become the inputs of PSR. Therefore the PSR, which was previously applied only to gaseous combustion systems, can now be implemented for biomass pyrolysis. It is a novel concept of predicting biomass pyrolysis in the sense of combining thermodynamic equilibrium and kinetic rate calculations. The aim of this study is to obtain more realistic pyrolysis end products in gas phase using PSR simulation at the same temperature of HSC calculation.

2. Materials and thermodynamic simulation results

Proximity and ultimate analysis results of three palm oil wastes (shell, fiber and empty fruit bunches – EFB) were obtained, as shown in Table 1, by a thermogravimetric analyser (TGA) (modeled TA 2050, USA) and CHNS/O Analyser (Perkin Elmer 2400II). Palm oil wastes contain very high volatile (>70 wt.%) and low fixed carbon (<20 wt.%). According to the ultimate analysis, palm oil wastes contain around 50 wt.% carbon and quite high oxygen (36–40 wt.%). The contents of nitrogen and sulfur in the palm oil wastes are close to zero (N: nearly zero; S: about 0.6 wt.%), and the ash content is also very low, mostly below 5 wt.%. If only considering the main elements (C, H, O), the molecular formula of the studied samples based on one C atom can be written as CH_xO_y, as listed in the last column of Table 1. Pyrolysis of the palm oil wastes was performed in TGA, and the gas products were on-line analysed using Fourier transform infrared spectroscopy (FTIR) (BioRad

Table 1
Proximate and ultimate analyses of palm oil wastes

	Proximate analysis (wt.%)				Ultimate analysis (wt.%)					LHV (MJ/kg)	Molecular formula
	M_{ad}	V_{ad}	A_d	FC_{ad}	C	H	N	S	O[a]		
Fiber	6.56	75.99	5.33	12.45	50.27	7.07	0.42	0.63	36.28	20.64	$CH_{1.69}O_{0.54}$
Shell	5.73	73.74	2.21	18.44	53.78	7.20	0.00	0.51	36.30	22.14	$CH_{1.61}O_{0.51}$
EFB	8.75	79.67	3.02	8.80	48.79	7.33	0.00	0.68	40.18	18.96	$CH_{1.80}O_{0.62}$

M: moisture content, V: volatile matters, A: ash, FC: fixed carbon; ad: on air dried basis; d: on dry basis.

[a] The O content was determined by difference.

Table 2
Yields of gas products from palm oil wastes pyrolysis (200–500 °C)

	Sample		Total relative area of absorbance peaks (area unit/g of waste)				
	H/C	O/C	CO_2	Organics	CH_4	CO	H_2O
Fiber	1.69	0.54	72,239	184,425	27,489	2902	44,474
Shell	1.61	0.51	74,561	194,734	25,358	3309	47,704
EFB	1.80	0.62	82,260	82,260	23,339	4879	48,525

Excalibur Series, model FTS 3000) with a deuterated triglycine sulfate (DIGS) detector which is connected to TGA. During TGA measurement, the buffer gas used is nitrogen and purge gas used for protection of balance is also nitrogen. As a result the yields of gas products were obtained from palm oil wastes pyrolysis in the temperature range of 200–500 °C as shown in Table 2. Yields of CO_2, CO, and H_2O from EFB are the highest among the three wastes while the highest CH_4 yield is found with fiber and the highest organic yield with shell, due to possibly their different components. Here, organics is a mixture of some acids, aldehydes, alkanes, and ethers. They are possibly formaldehyde (CH_2O), acetaldehyde (CH_3CHO), methanol (CH_3OH), formic acid (HCOOH), phenol (C_6H_5OH), acetone (CH_3COCH_3), etc.

Moreover, the HSC Chemistry performs the thermodynamic simulation of biomass pyrolysis using the values of ultimate analysis in Table 1. The first thermodynamic calculation considered the elements C, H, O, N, S and ~50 species, and furthermore simplified systems containing only C, H, O bearing species were investigated. Nitrogen as buffer and purge gases in TGA measurement were also first considered in HSC simulation and it was then found no influence of N_2 to the whole calculation system. Details are iterated in our previous publication [2]. The HSC calculations enable to simulate chemical reaction and processes on thermochemical basis. They utilize the principle that at equilibrium the total Gibbs energy of a system is at minimum to predict the equilibrium state. The results are shown in Fig. 1. The fiber sample was selected as a representative; its molar form is $CH_{1.69}O_{0.54}$ as seen from Table 1. The pyrolysis of palm oil wastes could be divided into four temperature zones separated by three vertical dot lines (see Fig. 1). In the first zone ($T < 340$ °C), biomass becomes dehydrated at this temperature, and along with water vapor, CO_2 and volatile organics (CH_4) are given off. The second zone is for temperature at 340–560 °C. Contents of CH_4 and water are decreased in Zone 2 but CO_2 content increased, carbon content keeps almost constant. There is also some H_2 and CO evolving out. In Zone 3 (560 °C < T < 900 °C), the secondary thermoanalysis happens. Contents of H_2 and CO are increased sharply. During the last zone (>900 °C), pyrolysis reaches the end. Almost no reaction occurs. The contents of H_2 (45 mol%) and CO (30 mol%) keep high and stable. Carbon residue is regarded as charcoal formed due to carbonization.

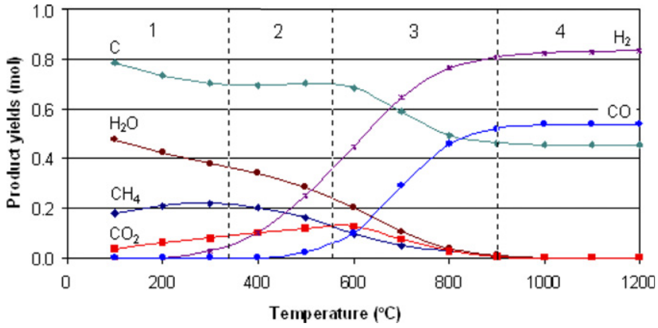

Fig. 1. HSC calculation for fiber pyrolysis.

However, the HSC calculations do not take into account kinetics (rates) of the chemical reactions and nonideality of solutions. The calculation does not give the reaction time that is necessary for the theoretical equilibrium state to be reached. Because the HSC calculation merely represents the compositions of pyrolysis in its most stable state, the end products (H_2, CO, CO_2, CH_4 and H_2O) did not contain unstable species like C_2H_2, C_2H_4, C_2H_6 and C_3H_8 which appear in modern biomass fast pyrolysis [25]. Therefore, the integrated effect of combining thermodynamic and kinetic concerns in biomass pyrolysis for a precise prediction of gas product distribution is meaningful.

3. Kinetic simulation of biomass pyrolysis

3.1. Model description

PSR stands for perfectly stirred reactor. The stirred reactor consists of a small thermally insulated chamber that has inlet and outlet ducts. A steady flow of fuel and oxidizer are introduced in such a way that high-intensity turbulent mixing causes the contents of the reactor to be nearly spatially uniform. This means that the rate of conversion from the reactants to produces is controlled by chemical reaction rates and not by mixing processes. The reactor requires fast mixing, and residence time has to be deduced from the flow rate and the reactor volume. The PSR code is designed to run in conjunction with CHEMKIN program, which handles the chemical reaction mechanism and the thermodynamic properties [22].

The PSR is programmed to predict steady-state temperature and species composition in a perfectly stirred reactor. The reactor is characterized by a reactor volume, residence time or mass flow rate, heat loss or temperature, and incoming temperature and mixture composition. This combustion program becomes thermal pyrolysis program when it is applied to combustion without oxidizer.

The concept of the PSR is shown in Fig. 2. The species conservation equation is given by

$$\dot{m}(Y_k - \overline{Y}_k) - \dot{\omega}_k W_k V = 0 \qquad (1)$$

and conservation of energy is stated as

$$\dot{m}\sum_{k=1}^{K}(Y_k h_k - \overline{Y}_k \bar{h}_k) + Q = 0. \qquad (2)$$

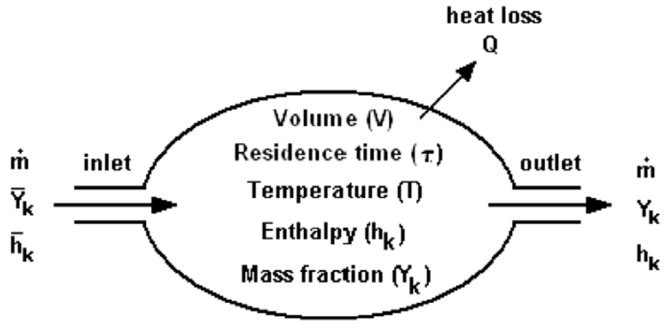

Fig. 2. Schematic representation of PSR.

In these equations Y_k is the mass fraction of the kth species; W_k, the molecular weight of the kth species; V, the reactor volume; $\dot{\omega}_k$, the molar rate of production by chemical reaction of the kth species per unit volume; h_k, the specific enthalpy of the kth species; and Q, the reactor heat loss. The $\overline{Y}_k$ and $\bar{h}_k$ represent inlet mass fraction and inlet enthalpy.

The normal residence time (τ) is related to the reactor volume (V) and the mass flow rate ($\dot{m}$) by

$$\tau = \frac{\rho V}{\dot{m}}, \tag{3}$$

where the mass density ρ is calculated from the ideal gas equation of state.

$$\rho = \frac{P\overline{W}}{RT}. \tag{4}$$

Here P is the pressure, T is the temperature, R the universal gas constant and $\overline{W}$ the mixture's mean molecular weight. The residence time is often used as a characteristic parameter of the reactor rather than the mass flow rate. When this is the case, $\dot{m}$ is computed from Eq. (3).

The net chemical production rate $\dot{\omega}_k$ of each species results from a competition between all the chemical reactions involving that species. Each reaction proceeds according to the law of mass and the forward rate coefficients are in the modified Arrhenius form

$$k_{\mathrm{f}} = AT^{\beta}\exp\left(\frac{-E_{\mathrm{A}}}{RT}\right). \tag{5}$$

Eqs. (1) and (2) form a set of $K+1$ nonlinear algebraic equations, the solution of which is the temperature and mass fractions. Even though the PSR program seeks the solution to the steady state equations, the computational algorithm often requires transient equations of mass conservation and energy conservation. Nevertheless, the transient equations are omitted here.

The PSR program for the biomass pyrolysis utilizes a detailed kinetic reaction mechanism. The most widely used detailed kinetic mechanism for hydrocarbon combustion is GRI mechanism which is developed by Gas Research Institute [26]. GRI mechanism is a list of elementary chemical reactions and associated rate constant expressions. Most of the reactions listed have been studied one way or another in the laboratories, and so the rate constant parameters mostly have more or less direct measurements behind them. Garg et al. utilized GRI-2.11 successfully with PSR for hydrocarbon-hydrogen reaction modeling [20]. The newest version of the mechanism is GRI-Mech III [26], which is a compilation of 325 elementary chemical reactions and associated rate coefficient expressions and thermochemical parameters for the 53 species involved in them.

In our analysis of volatile component in biomass pyrolysis there are 219 elementary chemical equations with 34 species of C/H/O system. The involved 34 species and 219 elementary equations are extracted from the C/H/O/N/Ar system of GRI-Mech III. The excluded species and elementary equations are nitrogen-driven and argon species and elementary equations. Table 3 shows all species included in the PRS calculations.

3.2. PSR calculations – system design

In our previous study [2] biomass decomposition was simplified as 'Biomass = $H_2 + CO + CO_2$ + hydrocarbon + charcoal', in which charcoal remained to be a solid as temperature above 1000 °C in HSC calculations. The representative expression of the HSC calculation in this study was obtained as $CH_{1.69}O_{0.54}$ for fiber palm oil wastes as shown in Table 1. However this expression cannot be used directly into the PSR program because it contains solid phase carbon (char), which was not allowed to enter as input into PSR. It was verified in the HSC calculations that the pyrolyzed gas components are different under different temperature conditions. In order to apply the HSC result more reasonably to PSR program, the charcoal has to be eliminated. As shown in Fig. 1, the molar content of carbon element (C) becomes constant at 0.46 when pyrolysis temperature is above ~1000 °C. The carbon molar

Table 3
Species considered in the C/H/O model

Species no.		Species no.		Species no.		Species no.		Species no.	
1	H_2	8	C_2H	15	CH_2	22	C_3H_7	29	CH_2O
2	O_2	9	C_2H_4	16	CH_4	23	CH_3CHO	30	CH_3OH
3	HO_2	10	HCCO	17	HCO	24	O	31	C_2H_3
4	CH	11	CH_2CHO	18	CH_3O	25	H_2O	32	C_2H_6
5	CH_3	12	H	19	C_2H_2	26	C	33	HCCOH
6	CO_2	13	OH	20	C_2H_5	27	CH_2	34	C_3H_8
7	CH_2OH	14	H_2O_2	21	CH_2CO	28	CO		

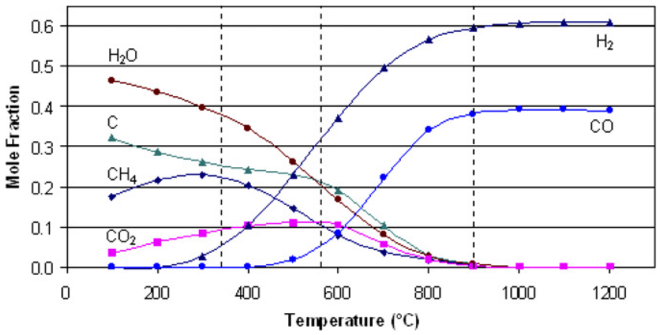

Fig. 3. Normalized HSC results after subtracting 0.46 from C.

content 0.46 is known as char and this remains to be a solid as the temperature rises further. The balance carbon by subtracting 0.46 from the original carbon content is known as volatile carbon, which can be entered into the PSR program. As such, a new figure (Fig. 3) is drawn after subtracting 0.46 from carbon content of Fig. 1. In Fig. 3 the y-axis represents mole fraction of individual species. HSC calculation is based on 1 mole of fiber palm oil waste as input value, thus the calculation leads to molar values of species in pyrolysis as shown in Fig. 1 taken from previous paper [1]. However, PSR calculation is designed to use mole fractions as input data, and the results yield also mole fractions of species. The result of HSC calculations, product yields in Fig. 1, was converted to mole fraction values in Fig. 3 for PSR calculation.

In applying the PSR code all characteristic parameters were derived from the TGA–FTIR reactor configuration, i.e., PSR reactor volume was 2.0 cm^3 and mass flow rate was 0.02 g/min. Although TGA is not exactly a steady flow of fuel system, the instant gas production rate can be obtained from the real-time FTIR scans (one IR spectrum was obtained in each 5 s) and therefore, the averaged mass flow rate of PSR was calculated based on it. The experimental reactor volume was 12 cm^3 through which biomass gas and purge gas (nitrogen) flow. The averaged portion of the biomass gas generated in the reactor was about 1/6 of total gas flow, which made the PSR reactor volume 2.0 cm^3. The biomass mass loss rate, which produced gas flow rate of PSR, is a function of temperature. In applying to PSR, mass flow rate of 0.02 g/min was calculated as experimental average value taken from TGA biomass loss rate in the reactor. Residence time was calculated by the program. The residence time for fiber pyrolysis was longest as 3.37 s at 100 °C of pyrolysis temperature and decreased with increasing pyrolysis temperature showing 0.72 s at about 1000 °C of pyrolysis temperature. Equivalence ratio is defined as follows: if f denotes the ratio of mass of fuel to the mass of oxidizer in a reactive mixture, the equivalence ratio, ϕ, is

$$\phi \equiv \frac{f}{f_s}, \tag{6}$$

where f_s is stoichiometric mass ratio [27]. In order to simulate the pyrolysis, the equivalence ratio was taken as 100, i.e., $\phi = 100$, which means that the molar value of fuel is 100 times bigger than the molar value of fuel necessary for stoichiometric reaction. A much higher equivalence ratio $\phi = 1000$ was also tested for the PSR calculations. The yielded components obtained by these two equivalence ratios showed negligible difference, i.e., less than 2% for each component.

Now the ideal implementation of PSR would be to use a fixed set of input components of biomass. For example, if the components of biomass obtained from HSC at 490 °C could be used as input values throughout all the temperature ranges, it would be desirable. However, HSC results showed that there is no representative component applied to the whole temperature region.

In the previous section of HSC calculations there were four distinct regions of pyrolysis gas products, i.e., $T <$ 340 °C, 340 °C $< T <$ 560 °C, 560 °C $< T <$ 900 °C and $T >$ 900 °C. Therefore the following equations are proposed to examine the HSC results of fiber for each temperature range, based on the major products predicted by HSC (see Fig. 1):

(1) For $T <$ 340 °C:

$$CH_{1.69}O_{0.54} \rightarrow 0.75C + 0.45H_2O + 0.2CH_4 + 0.05CO_2$$

(2) For 340 $< T <$ 560 °C:

$$\begin{aligned} CH_{1.69}O_{0.54} \rightarrow\ & 0.70C + 0.32H_2O + 0.18CH_4 \\ & + 0.16H_2 + 0.11CO_2 \end{aligned}$$

(3) For 560 $< T <$ 900 °C:

$$\begin{aligned} CH_{1.69}O_{0.54} \rightarrow\ & 0.56C + 0.69H_2 + 0.35CO + 0.08H_2O \\ & + 0.05CO_2 + 0.03CH_4 \end{aligned}$$

(4) For $T >$ 900 °C:

$$CH_{1.69}O_{0.54} \rightarrow 0.46C + 0.84H_2 + 0.54CO$$

As explained earlier in this section, the nonvolatile portion of biomass (= 0.46 C) is subtracted from the above component descriptions for each temperature range to be used as input values to PSR. The representative species concentrations in each region were chosen at mid-point of the region, i.e., 175 °C, 550 °C, 730 °C and 1050 °C shown in Fig. 3 in which the species concentrations were normalized as mole fractions. A typical PSR result is shown in Fig. 4 with main product species from biomass pyrolysis occurring at 490 °C. It can be seen that all N-driven species and Ar species become zero in concentration, as there should be negligible N and Ar containing species generated in the course of pyrolysis.

3.3. PSR calculation results

The normalized results of PSR calculations are shown in Fig. 5. As expected in earlier section, the concentration of

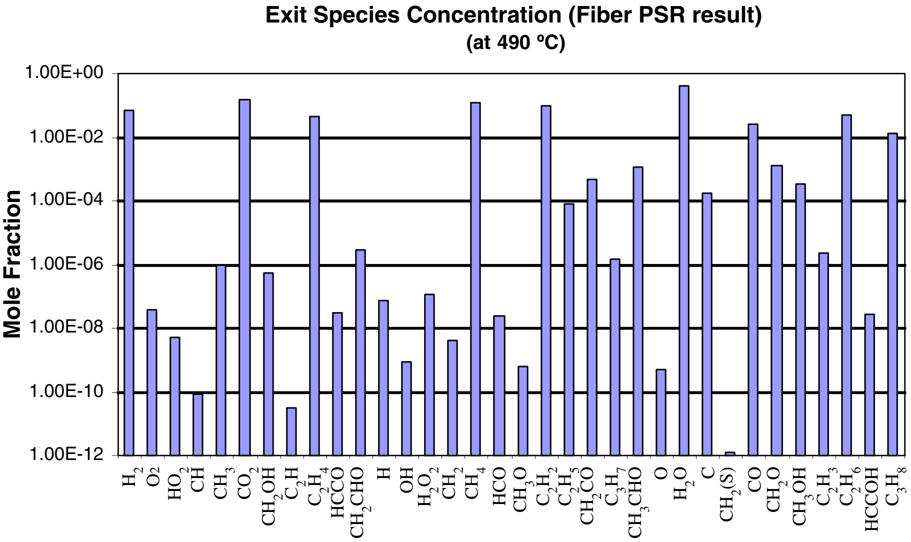

Fig. 4. Exit species concentration at 490 °C.

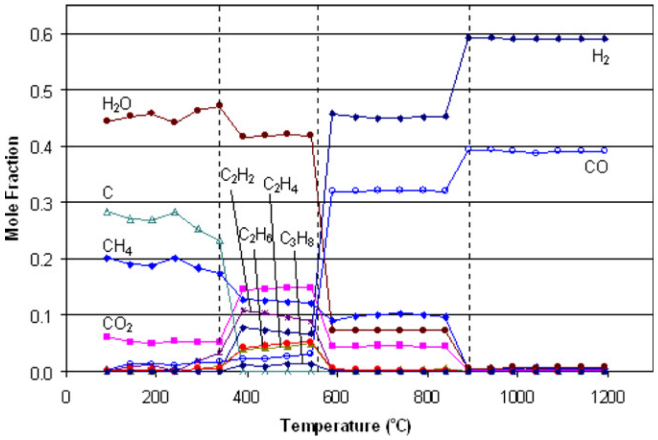

Fig. 5. Normalized PSR results for 4 representative species concentration application.

Table 4
PSR input values calculated from HSC (moles)

Temperature (°C)	C	C – 0.46	H_2O	CH_4	CO_2	H_2	CO
100	0.785	0.33	0.475	0.18	0.035	0	0
200	0.735	0.28	0.425	0.21	0.06	0	0
300	0.705	0.25	0.38	0.22	0.08	0.025	0
400	0.695	0.24	0.34	0.2	0.1	0.1	0
500	0.705	0.25	0.285	0.16	0.12	0.25	0.02
600	0.685	0.23	0.2	0.095	0.125	0.445	0.1
700	0.59	0.135	0.105	0.05	0.075	0.645	0.29
800	0.495	0.04	0.035	0.025	0.025	0.765	0.46
900	0.465	0.01	0.01	0.005	0.005	0.81	0.52
1000	0.455	0	0	0	0	0.825	0.535
1100	0.455	0	0	0	0	0.83	0.535
1200	0.455	0	0	0	0	0.835	0.535

C species becomes zero instantly in the second zone (340 °C < T < 560 °C). When this figure is compared with HSC result in Fig. 3, the PSR results tend to be flat in each region showing severe disconnections at each boundary temperature. This tendency became clearer at higher temperature regions. This might explain that PSR application is more sensitive to input component than temperature. At the second temperature region of 340–560 °C, the figure shows new species C_2H_2, C_2H_6, C_2H_4, and C_3H_8 in the range of 11–1.5% mole fractions. These newly generated species shows more realistic pyrolysis.

Another scheme to apply PSR for pyrolysis is to use the HSC species mole fractions obtained at each point of temperature. The input values are shown in Table 4. All the components were calculated from 100 °C to 1200 °C stepping up by 100 °C, i.e., normalized HSC results after subtracting the 0.46 moles from the original carbon contents. This table represents all the gaseous components and volatile carbon that can be entered into the PSR program at each temperature. The results of PSR calculations are shown in Fig. 6. The different outputs shown in Figs. 5

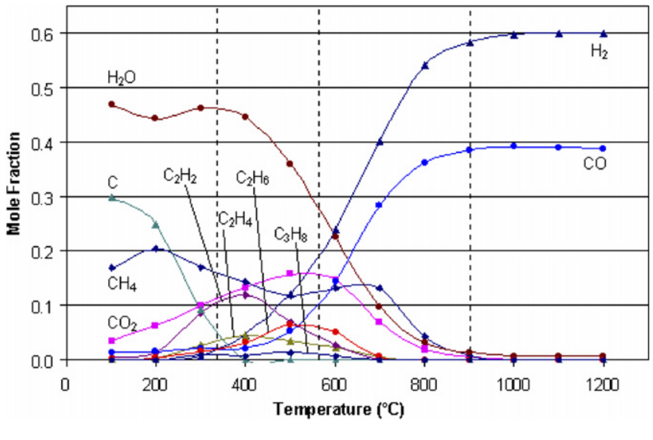

Fig. 6. Normalized PSR results for each point species concentration application.

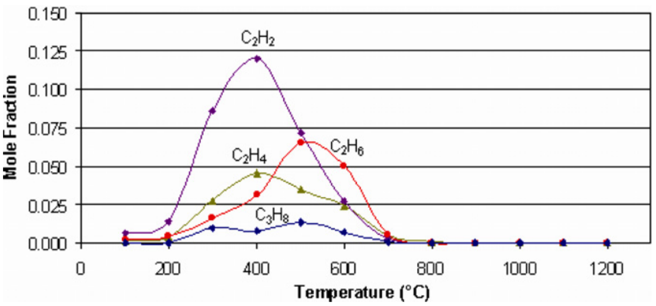

Fig. 7. Details of newly evolved species taken from normalized PSR results.

and 6 resulted from different input manners from HSC to PSR. The regional input, from which Fig. 5 was generated, was performed to examine whether representative gas phase components could be applied to the region. In a region, as inputs the gas phase components were fixed and temperature were variable within the region. Another scheme of choosing input values for PSR, from which Fig. 6 was generated, was to use the gas phase components (i.e., HSC species mole fractions) obtained at each point of temperature. In this case, the input values are variable temperature and gas phase components determined at that temperature by HSC.

There are again newly developed components, i.e., C_2H_2, C_2H_6, C_2H_4, and C_3H_8 in the range of 12–1.4% and they were obtained in the price of reducing the amount of all original components of HSC pyrolysis. The details of newly evolved species are shown in Fig. 7 in bigger scales. Most of the species were evolved in the temperature range of 200–700 °C. C_2H_2 started to evolve at earliest stage of about 150 °C, maximum at about 400 °C, and diminished at about 700 °C. C_2H_6 is slow to reach peak point than C_2H_2 and C_2H_4. All four species diminished to evolve at about 700 °C. C_2H_2 evolved as the biggest component as 12% of mole fraction at about 400 °C and C_2H_4 shows 4.5% mole fraction at the same temperature. Second biggest yielded component is C_2H_6 with 6.5% of mole fraction at about 500 °C and C_3H_8 has maximum yield value of 1.4% mole fraction at the same temperature. There are two peak points for C_3H_8 while only one peak point for other newly evolved species.

When this individual input method (Fig. 6) is applied, the discontinuities between each region (divided by dotted lines in the figure) no more exist. The regional input method (Fig. 5) shows no change in species output especially in higher temperature regions (560 °C $< T <$ 900 °C, $T >$ 900 °C).

If comparing the PSR results (Fig. 6) with HSC results (Fig. 3), Fig. 6 shows the mole fraction of H_2O starts to increase at about 200 °C becomes maximum at about 300 °C, and then decreases, while the HSC result (Fig. 3) has constantly decreasing tendency. The biggest contributors to newly evolved species evolution (C_2H_2, C_2H_4, C_2H_6 and C_3H_8) are C and CH_4 in the region of 200 °C to 700 °C. During this evolution period the mole fraction of C diminished quickly and at about 400 °C the mole fraction became zero, and CH_4 started to diminish at about 200 °C but slowly until 500 °C, and then increased slightly up to about 700 °C. In Fig. 3 of HSC results both C and CH_4 diminishes slowly. At above about 800 °C the output species H_2 and CO remains the same in both PRS results and HSC results.

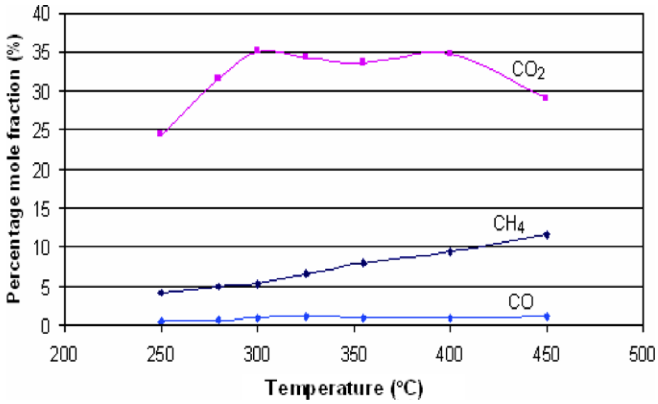

Fig. 8. Gas products releasing profiles from fiber pyrolysis.

To compare the prediction with experimental results, we need to know the molar fraction of each gas in total. Unfortunately H_2 cannot be detected by FTIR, although it should be presenting in the gas products (see Table 2) [2]. In our following work, MicroGC was used to measure all the gas species and obtain the molar fraction of each in total. From FTIR analyses of this study, only the concentration of CO_2, CO and CH_4 were calibrated but excluding organics as it covers several species. As a result, the relative molar percentage based on IR areas detected was adopted to estimate the percentage molar fraction of gas products and the results from fiber pyrolysis are shown in Fig. 8. The real pyrolysis of fiber in TGA system (Fig. 8) happened at lower temperatures (250–450 °C) compared to the simulation (Fig. 6). The changing patterns of CO_2 from experiment and simulation are quite similar but those for CO and CH_4 are different, due to most likely certain limitations of TGA as a reactor system.

4. Conclusions

Our previous work involved experimental study using TGA–FTIR and thermodynamic modeling (HSC) of gas product yielding, and both indicate the similar results: total gas yield is increased with temperature at the expense of char residue. However, due to the deficiency of kinetic characteristics of HSC calculations, the yielded products overlooked many hydrocarbon gases that appear in modern fast biomass pyrolysis process. Implementing a combustion code PSR coupled with HSC results made the final gas products more realistic.

The PSR modeling made it possible to have additional gas products such as C_2H_2, C_2H_4, C_2H_6 and C_3H_8, and they were obtained in the price of reducing the amount of all original products of HSC pyrolysis, especially volatile portion of C and CH_4. Most of the new species were evolved in the temperature range of 200–700 °C. C_2H_2 is yielded as the biggest component as 12% of total mole fraction at 400 °C and C_2H_4 shows 4.5% mole fraction at the same temperature. Second biggest yielded component is C_2H_6 (6.5%) at about 500 °C and C_3H_8 (1.4%) has maximum yield value at the same temperature.

In conclusion, PSR demonstrated as powerful tool for simulation of biomass pyrolysis when coupled with HSC calculation. However, this work is just a first step; further studies are needed in applying PSR in other reactor applications of biomass pyrolysis/gasification for a better/closer prediction to the reality.

References

[1] Yang H, Yan R, Chin T, Liang DT, Chen HP, Zheng CG. Thermogravimetric analysis – Fourier transform infrared analysis of palm oil waste pyrolysis. Energy Fuels 2004;18:1814–21.

[2] Yan R, Yang H, Chin T, Liang DT, Chen H, Zheng CG. Influence on the temperature on the distribution of gases products from pyrolyzing palm oil wastes. Combust Flame 2005;142:24–32.

[3] Iwasaki W. A consideration of the economic efficiency of hydrogen production from biomass. Int J Hydrogen Energy 2003;28:939–44.

[4] Babu BV, Chaurasia AS. Pyrolysis of biomass: improved models for simultaneous kinetics and transport of heat, mass and momentum. Energy Convers Manage 2004;45:1297–327.

[5] Rostami AA, Hajaligol MR, Wrenn SE. A biomass pyrolysis submodel for CFD applications. Fuel 2004;83:1519–25.

[6] Varhegyi G, Antal MJJ, Jakab E, Szabo P. Kinetic modeling of biomass pyrolysis. J Anal Appl Pyrolysis 1997;42:73–87.

[7] Jensen PA, Frandsen FJ, Dam-Johansen K, Sander B. Experimental investigation of the transformation and release to gas phase of potassium and chlorine during straw pyrolysis. Energy Fuels 2000; 14:1280–5.

[8] Gueret C, Daroux M, Billaud F. Methane pyrolysis: thermodynamics. Chem Eng Sci 1997;5:815–27.

[9] Fink JK. High temperature pyrolysis of plastics in contact with liquid steel. J Anal Appl Pyrolysis 1999;49:107–23.

[10] Lee YL, Sanchez JM. Theoretical study of thermodynamics relevant to tetramethylsilane pyrolysis. J Cryst Growth 1997;178:513–7.

[11] Zainal ZA, Ali R, Lean CH, Seetharamu KN. Prediction of performance of a downdraft gasifier using equilibrium modeling for different biomass materials. Energy Convers Manage 2001;42: 1499–515.

[12] Li XT, Grace JR, Watkinson AP, Lim CJ, Ergüdenler A. Equilibrium modeling of gasification: a free energy minimization approach and its application to a circulating fluidized bed coal gasifier. Fuel 2001;80: 195–207.

[13] de Bruyn Kops SM, Malte PC. Final Technical Report to US Department of Energy: Simulation and modeling of wood dust combustion in cyclone burners, 2004.

[14] Philippe M, Raphael D. Performance analysis of a biomass gasifier. Energy Convers Manage 2002;43:1291–9.

[15] Baumlin S, Broust F, Ferrer M, Meunier N, Marty E, Lédé J. The continuous self stirred tank reactor: measurement of the cracking kinetics of biomass pyrolysis vapours. Chem Eng Sci 2005;60: 41–55.

[16] Liang XH, Kozinski JA. Numerical modeling of combustion and pyrolysis of cellulosic biomass in thermogravimetric systems. Fuel 2000;79:1477–86.

[17] Montgomery CJ, Cremer MA, Chen JY, Westbrook CK, Maurice LQ. Reduced chemical kinetic mechanisms for hydrocarbon fuels. J Propul Power 2002;18:192–8.

[18] Savage PE. Mechanisms and kinetics models for hydrocarbon pyrolysis. J Anal Appl Pyrolysis 2000;54:109–26.

[19] Strezov V, Lucas JA, Strezov L. Experimental and modelling of the thermal regions of activity during pyrolysis of bituminous coals. J Anal Appl Pyrolysis 2004;71:375–92.

[20] Garg RK, Gore JP, Fisher TS. Numerical simulation of hydrocarbon reaction chemistry in a CVD reactor. In: Proceedings of IMECE 2003, ASME international mechanical engineering congress, Washington, DC, 2003.

[21] Wu YG, Lin Y, Huang C. Kinetic study of the pyrolysis of tetrachloroethylene in a hydrogen rich environment. Fuel 2004;83: 2237–48.

[22] Glarborg P, Kee RJ, Grcar JF, Miller JA. PSR: a Fortran program for modeling well-stirred reactors (Sandia Report), USA, 1991.

[23] Zhou X, Mahalingam S. Evaluation of reduced mechanism for modeling combustion of pyrolysis gas in wildland fire. Combust Sci Technol 2001;171:39–70.

[24] Roine A. Outokumpu HSC chemistry for windows: chemical reaction and equilibrium software with extensive thermochemical database. HSC chemistry 4.0, Outokumpu Research Oy, Finland, June 1999, ISBN: 952-9507-05-04.

[25] Klass DL. Biomass for renewable energy, fuels, and chemicals. San Diego, USA: Academic Press; 1998.

[26] GRI Mech. Available from: http://www.me.berkeley.edu/gri_mech/index.html.

[27] Strahle WC. An introduction to combustion. USA: Gordon and Breach Science Publishers; 1993.